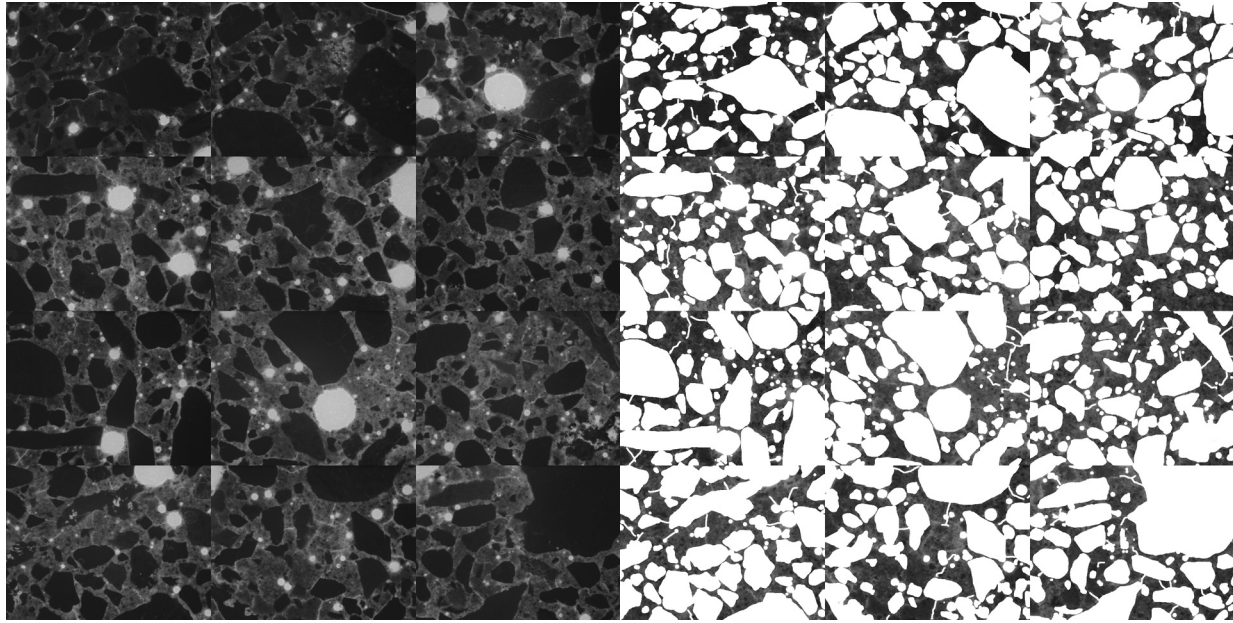


Figure 58: Mosaic of twelve images collected from the poor F-T performance LO-SYN-FA-6SK-45WC mixture (left), and after masking air-voids and sand to isolate fluorescence from the cement paste (right).

Table 26: Average fluorescence values measured in grey scale level from cement paste for each image collected from the poor F-T performance LO-SYN-FA-6SK-45WC mixture, and correlated equivalent w/cm values based on calibration curve.

Avg. intensity of individual images (grey scale level)				Equiv. w/cm based on 28d mortar stds.			
108	92	99	97	0.51	0.44	0.47	0.46
95	89	105	119	0.45	0.42	0.49	0.56
112	105	101	94	0.53	0.49	0.48	0.45
Average				0.48	Std. dev.	0.04	

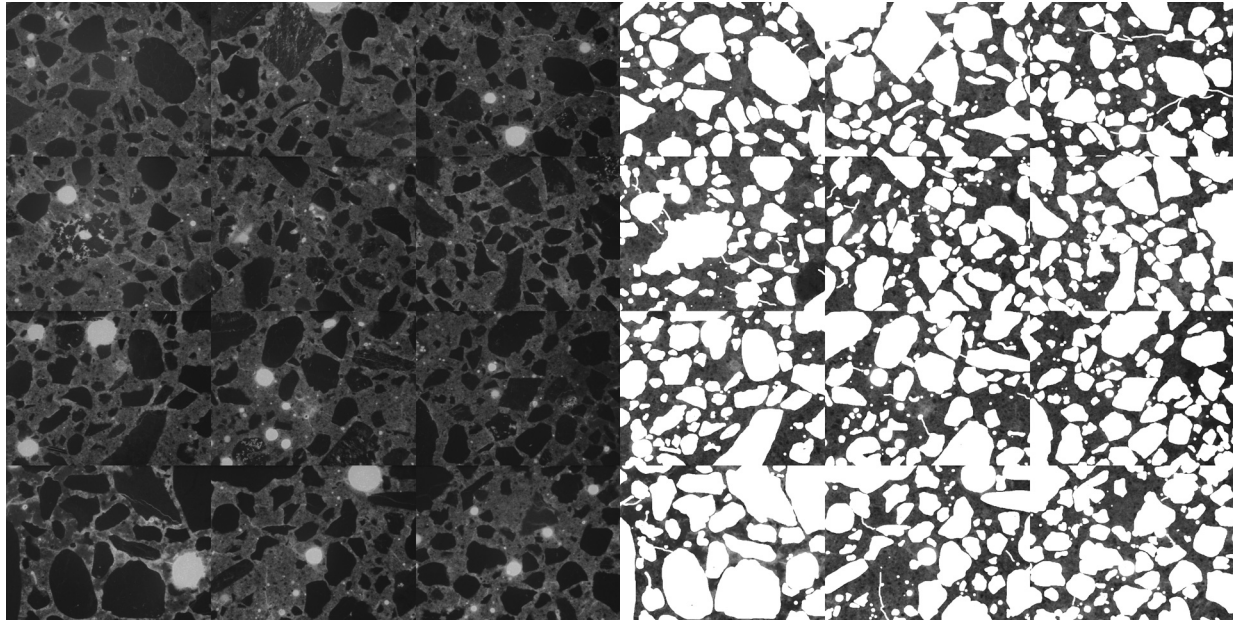


2.0 mm

Figure 59: Mosaic of twelve images collected from the normal set LO-VR-SLG-6SK-45WC mixture (left), and after masking air-voids and sand to isolate fluorescence from the cement paste (right).

Table 27: Average fluorescence values measured in grey scale level from cement paste for each image collected from the normal set LO-VR-SLG-6SK-45WC mixture, and correlated equivalent w/cm values based on calibration curve.

Avg. intensity of individual images (grey scale level)				Equiv. w/cm based on 28d mortar stds.			
46	50	64	76	0.24	0.25	0.31	0.37
76	61	62	81	0.37	0.30	0.31	0.39
74	74	65	68	0.36	0.36	0.32	0.33
				Average	0.33	Std. dev.	0.05



2.0 mm

Figure 60: Mosaic of twelve images collected from delayed set LO-SYN-SLG-6SK-45WC mixture (left), and after masking air-voids and sand to isolate fluorescence from the cement paste (right).

Table 28: Average fluorescence values measured in grey scale level from cement paste for each image collected from the delayed set LO-SYN-SLG-6SK-45WC mixture, and correlated equivalent w/cm values based on calibration curve.

Avg. intensity of individual images (grey scale level)				Equiv. w/cm based on 28d mortar stds.			
76	76	62	77	0.37	0.37	0.31	0.37
65	72	71	67	0.32	0.35	0.35	0.33
54	75	70	70	0.27	0.36	0.34	0.34
				Average	0.34	Std. dev.	0.03

5.2.6 Characterization of Cement for CEMHYD3D Modeling of Capillary Pore Structure

To investigate the utility of computer models in the interpretation and prediction of cement paste capillary porosity, the Lafarge Type I/II portland cement was characterized for input into the National Institute of Standards and Technology (NIST) CEMHYD3D v3.0 Cement Hydration and Microstructure Development Modeling Package [2005]. The characterization was performed in several steps, as outlined below.

5.2.6.1 Particle Size Distribution

Scanning electron microscope (SEM) back-scattered electron (BSE) images of portland cement dispersed on carbon tape were used to measure the particle size distribution. To disperse the cement, a small amount (approximately 0.01 g) was placed in the bottom of a plastic jar with a small hole in the side to accept a straw from a can of compressed air. A small piece of carbon

tape (approximately 1 cm²) was placed alongside the cement. The lid to plastic jar was secured, the straw was inserted, and a short blast of compressed air was used to send the cement airborne. After the cement had settled over the base of the jar (about a 2 minute wait), the carbon tape was removed from the jar, and a conductive layer of carbon was evaporated over the sample before placement in the SEM for imaging. A series of thirty images were recorded from the sample, at a pixel resolution of $0.171 \times 0.171 \mu\text{m}$. The digital images were analyzed in several steps, as outlined in Figure 61 using Image J, a public domain Java image processing program [2010]. First, a threshold was applied. Next, any “holes” in the particles were automatically filled, and particles touching the edge of an image were automatically removed. Finally, the particle profiles were automatically approximated by ellipses, and the minimum diameters (Feret diameters) used to define the particle sizes. A series of four different threshold levels were assessed, with total particle counts for the thirty images on the order of 5,000. The resulting particle size distributions are shown in Figure 62. As a compromise, an average particle size distribution based on the curves shown in Figure 62 was used for input into the CEMHYD3D model.

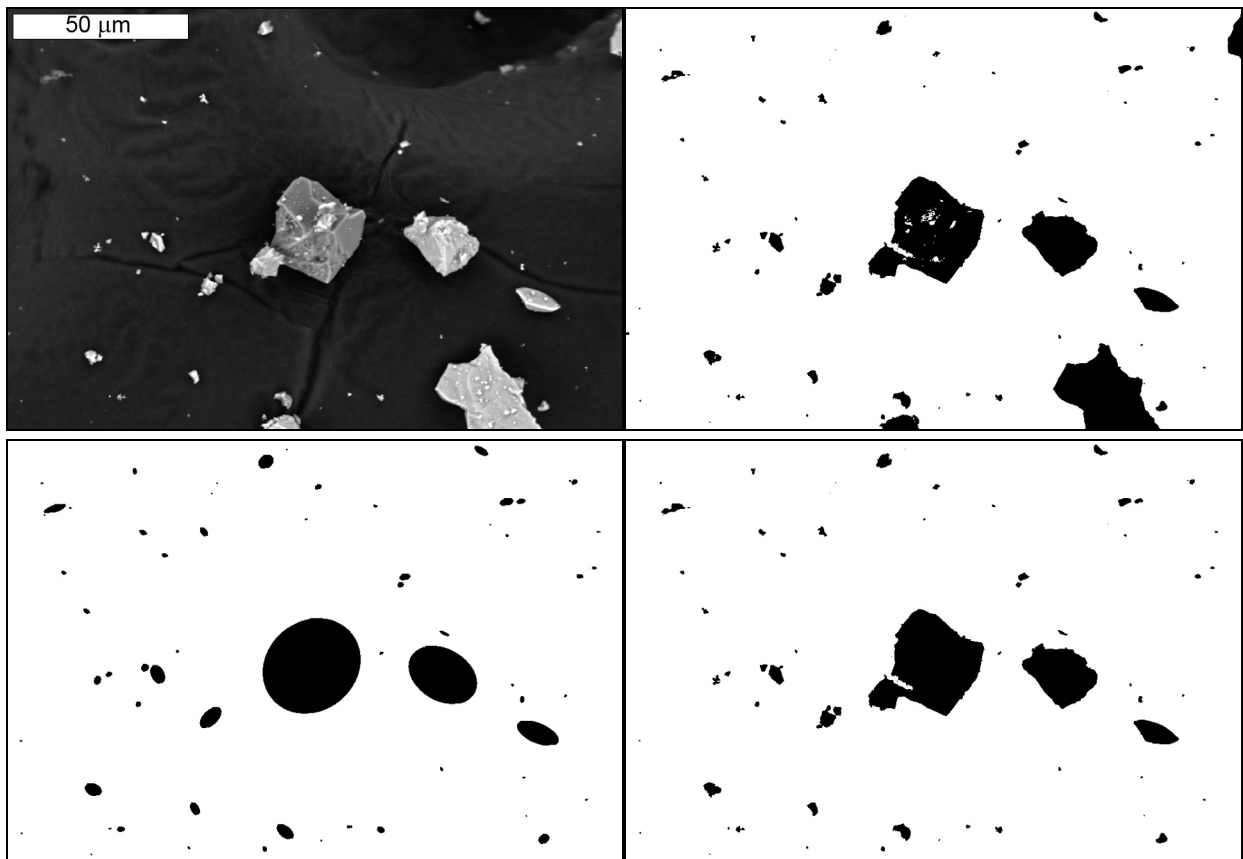


Figure 61: Clockwise from upper left: BSE image, binary image resulting from the application of a threshold of 85, after filling of holes and removal particles touching the edge, and approximation of particle profiles by ellipses.

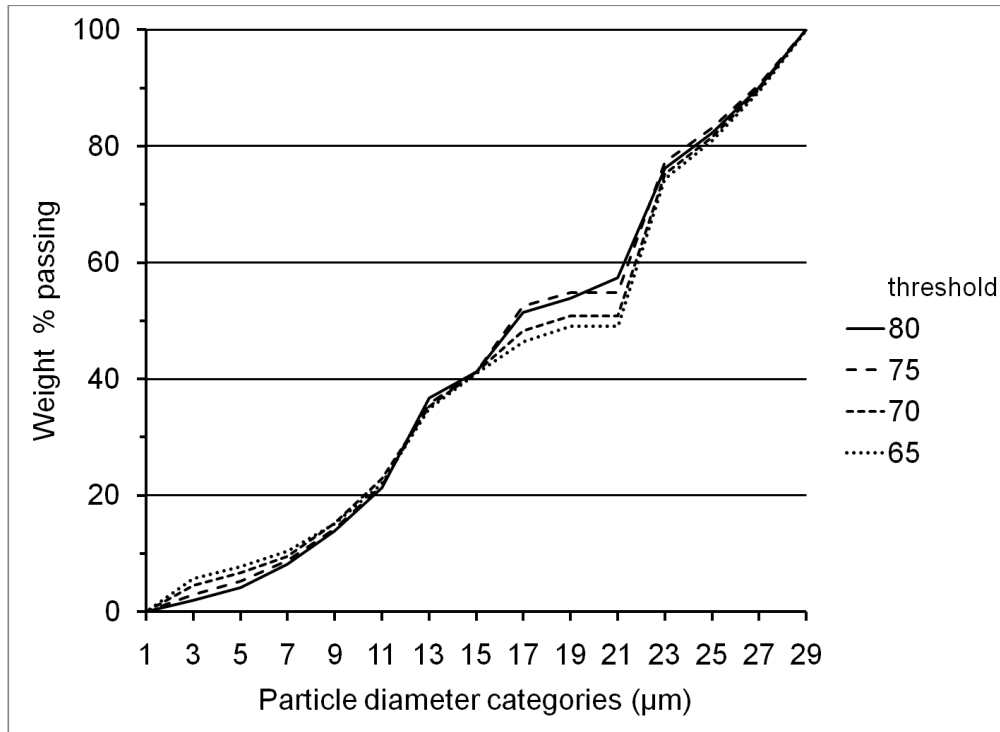


Figure 62: Portland cement particle size distributions as measured using different threshold levels.

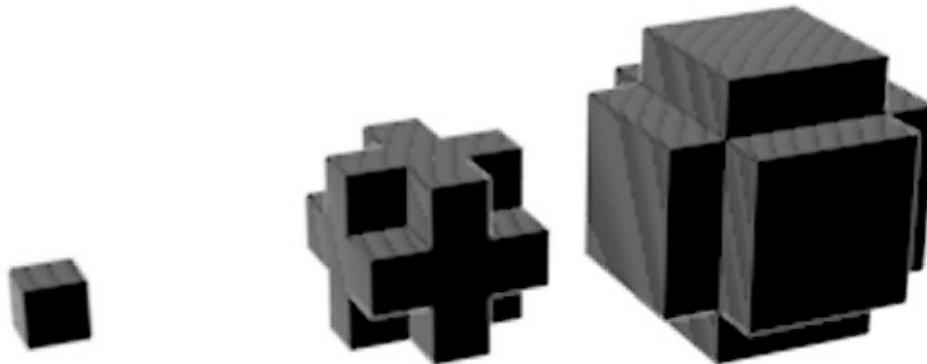


Figure 63: From left to right, depictions of voxelized spheres with diameters of 1, 3, and 5 voxels, and volumes of 1, 19, and 81 voxels respectively.

The CEMHYD3D model is based on voxels with dimensions of $1 \mu\text{m}^3$. Cement grains are approximated as voxelized spheres centered on a single pixel, which limits the dimensions of particles in the model to diameters of 1, 3, 5, 7 μm and so on. A depiction of voxelized spheres of diameters 1, 3, and 5 is included in Figure 63.

The CEMHYD3D program genpartnew.c was used to generate portland cement systems at w/cm levels of 0.45, 0.50, and 0.52 to parallel the laboratory concrete mixtures. Each scenario consisted of a 0.001 mm^3 (1 million voxel) cube populated by the correct number of cement grains (on the order of 15,000) to satisfy the required w/cm (with the spaces between particles

filled by water). For the Lafarge Type I/II cement used in the study, particles were categorized into one of three basic categories: cement grains, interground limestone, and interground calcium sulfate phases. The particle size distribution determination did not differentiate between these three categories, so when setting up the model parameters, it was assumed that the same particle size distribution applied to all three categories.

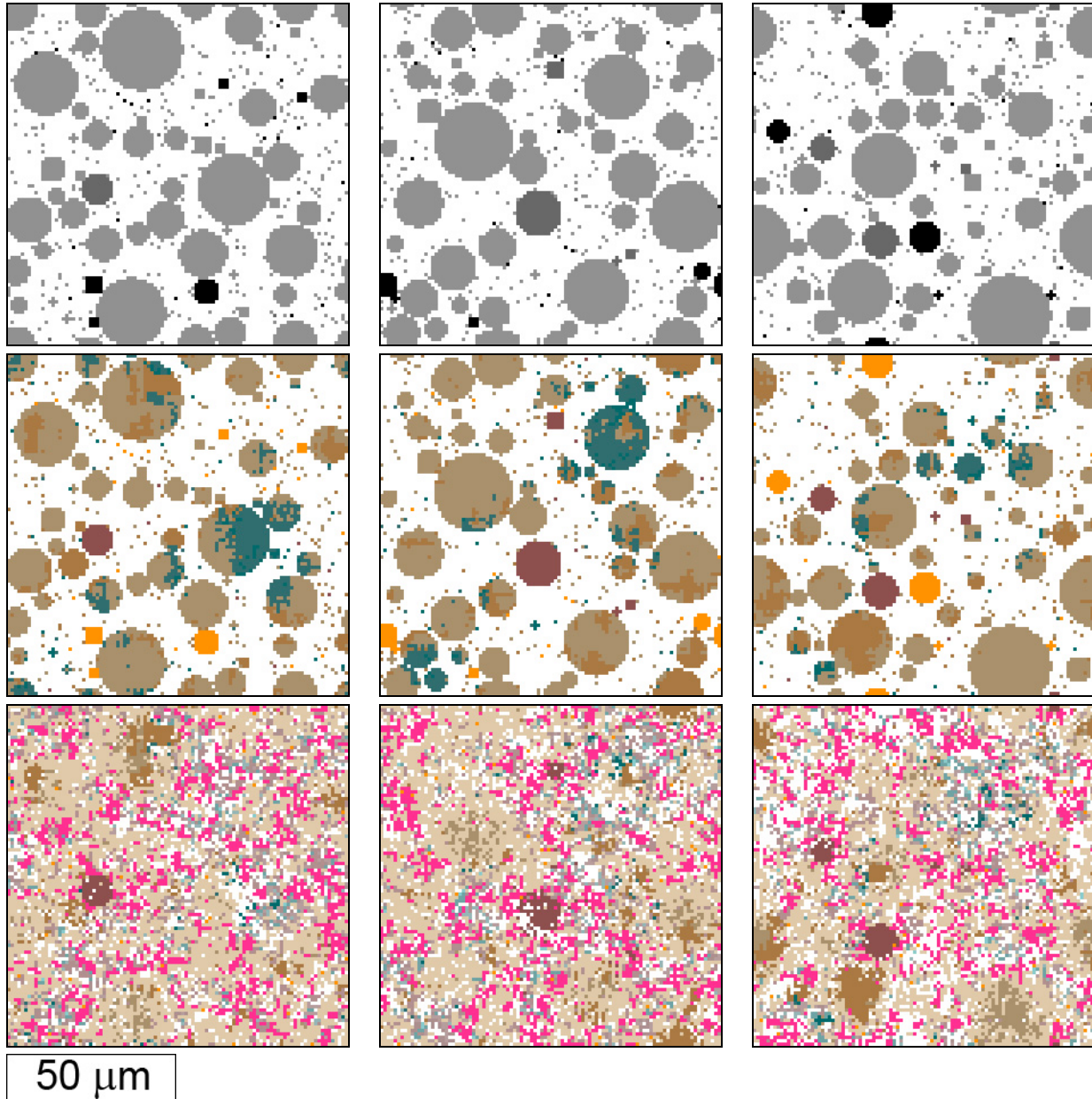


Figure 63: 2D slices from 3D models to illustrate steps in the CEMHYD3D process. From left to right: 0.45, 0.50, and 0.52 w/cm. Top row shows initial placement of particles where light gray = undifferentiated cement grains, dark gray = interground limestone, and black = interground calcium sulfate phases. Middle row shows particles partitioned into phases using same color scheme described in Figure 65. Bottom row shows hydrated system at 56 days, where C-S-H phases are light tan, Ca(OH)₂ is red, and aluminat hydrate phases are light blue-gray.

The volume fractions of limestone and calcium sulfate phases were estimated based on concentration data from the cement mill test report. Using a specific gravity of 2.59 for the Presque Isle limestone, the 3.7 wt. % limestone listed in the cement mill test report was converted to a volume of 4.5 wt. %. The SO₃ content of 2.5 wt. % listed in the cement mill test report was attributed solely to the presence of CaSO₄ at a corresponding concentration of 4.3 wt. %. Finally, it was assumed that the CaSO₄ phases consisted of equal volumes of gypsum and hemihydrate. Using the specific gravities of gypsum and hemihydrate (2.3 and 2.7 respectively) the corresponding volume fractions were computed at 3.1 % each. The top third of Figure 63 shows slices from the 0.45, 0.50, and 0.52 w/cm cubes output by genpartnew.c, and includes particles with a size of one voxel. Technically, the one-voxel-sized particles are not added until later in the CEMHYD3D modeling process.

5.2.6.2 Partitioning of Cement Clinker Particles into Cement Phases

A series of SEM x-ray energy dispersive spectroscopy (EDS) elemental maps were collected from a flat polished cross-section through a sample of Lafarge Type I/II portland cement that had been embedded in epoxy, as shown in Figure 64. The images shown in Figure 64 were imported into Multispec©, [2010], A Freeware Multispectral Image Data Analysis System, which was used to produce the classified image shown in Figure 65. In Figure 65 the image has been partitioned into the primary phases of portland cement. The CEMHYD3D program statsimp.c was used to extract the volume fraction and surface area fraction of alite (C₃S), belite (C₂S), tricalcium aluminate (C₃A), and tetracalcium aluminoferrite (C₄AF) phases from Figure 65. The CEMHYD3D program corrcalc.c was used to define the autocorrelation functions for the cement phases from Figure 65. The CEMHYD3D program corrx2r.c was used to translate the corrcalc.c output into polar coordinates. The output from these programs was used by the CEMHYD3D program distrib3d.c to partition the cement grains into cement phases. The middle portion of Figure 63 shows the cement grains after partitioning into the C₂S, C₃S, C₃A, and C₄AF phases.

5.2.6.3 Cement Alkalis

As shown in Figure 65, there is a K₂SO₄ component to the portland cement. To account for the presence of alkalis in the model, the total wt. % Na₂O and K₂O in the cement must be known, along with the wt. % of each that is readily soluble. The readily soluble alkalis in the cement were measured according to ASTM C114 Standard Test Methods for Chemical Analysis of Hydraulic Cement, Section 18.2 Water-Soluble Alkalis, and found to be 0.068 wt. % Na₂O and 0.292 wt. % K₂O. The total alkalis listed in the cement mill test report were reported as 0.50 wt. % Na₂O_{equiv.}, and not broken down into wt. % Na₂O and wt. % K₂O. The same ratio of Na₂O to K₂O as found in the test for water-soluble alkalis was used to partition the total wt. % Na₂O and K₂O of the cement (computed at 0.09 and 0.62 wt. % respectively). These estimated values, along with the measured water-soluble values, were input into the *alkalichar.dat* file used to run the CEMHYD3D model.

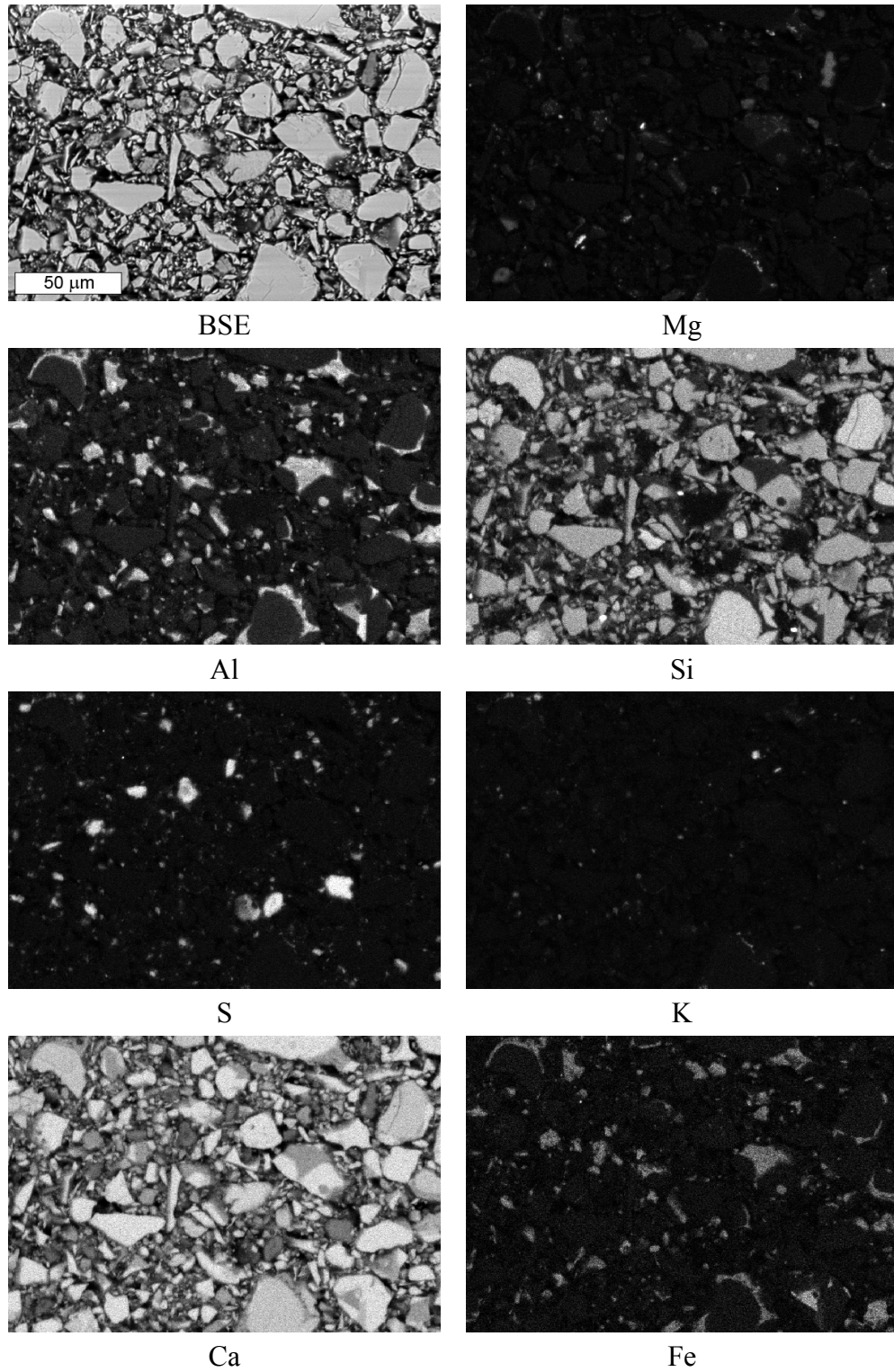


Figure 64: BSE image and elemental maps collected from polished cross-section through portland cement grains embedded in epoxy resin.